

E2HiL: Entropy-Guided Sample Selection for Efficient Real-World Human-in-the-Loop Reinforcement Learning

Haoyuan Deng¹, Yuanjiang Xue¹, Haoyang Du¹, Boyang Zhou¹, Zhenyu Wu², and Ziwei Wang^{1†}

Abstract— Human-in-the-loop guidance has emerged as an effective approach for enabling faster convergence in online reinforcement learning (RL) of complex real-world manipulation tasks. However, existing human-in-the-loop RL (HiL-RL) frameworks often suffer from low sample efficiency, requiring substantial human interventions to achieve convergence and thereby leading to high labor costs. To address this, we propose a sample-efficient real-world human-in-the-loop RL framework named **E2HiL**, which requires fewer human intervention by actively selecting informative samples. Specifically, stable reduction of policy entropy enables improved trade-off between exploration and exploitation with higher sample efficiency. We first build influence functions of different samples on the policy entropy, which is efficiently estimated by the covariance of action probabilities and soft advantages of policies. Then we select samples with moderate values of influence functions, where shortcut samples that induce sharp entropy drops and noisy samples with negligible effect are pruned. Extensive experiments on four real-world manipulation tasks demonstrate that **E2HiL** achieves a 42.1% higher success rate while requiring 10.1% fewer human interventions compared to the state-of-the-art HiL-RL method, validating its effectiveness. The project page providing code, videos, and mathematical formulations can be found at <https://e2hil.github.io/>.

I. INTRODUCTION

Robotic manipulation is a fundamental capability for robots deployed in both industrial assembly and household services [1], [2]. Despite decades of progress, achieving human-level manipulation skills in dynamic and unstructured environments remains a formidable challenge [3], [4]. Meanwhile, conventional manually designed controllers struggle to generalize across diverse tasks and high-dimensional policy spaces [5], motivating the transformation toward data-driven learning approaches.

Although pre-trained imitation policies show strong performance, they still struggle with out-of-distribution (OOD) states [6]–[10]. To improve robustness, recent work leverages RL’s trial-and-error exploration to acquire more reliable task-specific skills. However, RL trained purely in simulation often fails to transfer to real robots due to gaps in dynamics and perception [11], [12], prompting the adoption of real-world reinforcement learning. Nevertheless, directly training on real-world robots intensifies challenges such as low sample efficiency [13] and sparse rewards [14], [15]. Human-in-the-loop RL (HiL-RL) [3] leverages human corrective takeovers to accelerate online policy learning. However, existing human-in-the-loop RL methods still require extensive human intervention samples to converge, as the complexity

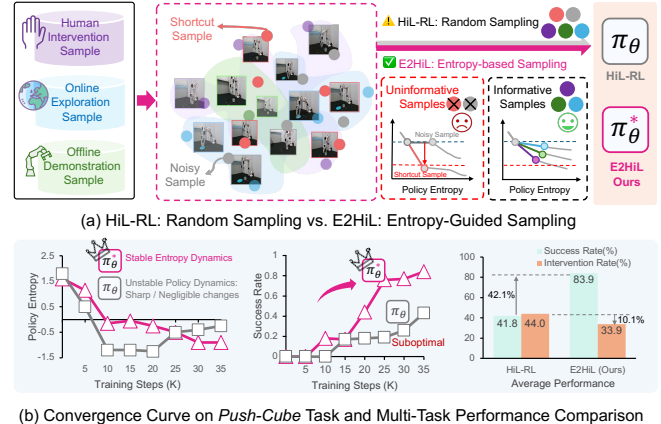


Fig. 1: Compared with random uniform sampling in HiL-RL, **E2HiL** avoids early entropy collapse through entropy-guided sample selection, achieving a better exploration–performance trade-off and improving success rates while reducing human costs.

of policy learning grows exponentially with the state–action dimensionality and task horizon, ultimately leading to high human labor costs [16]. This naturally raises the question: *How can we achieve more stable and sample-efficient human-in-the-loop RL in real-world robotic manipulation?*

In this paper, we propose an efficient real-world human-in-the-loop RL framework named **E2HiL** with active entropy-guided sample selection. Specifically, we identify a key limitation of existing HiL-RL methods: they cannot distinguish which intervention samples are truly informative, leading to inefficient use of human effort and degraded exploration. Fig. 1 reveals a clear trade-off between entropy dynamics and policy improvement during HiL-RL training. This pattern mirrors recent LLM-RL findings [17], [18], where rapid entropy reduction leads to premature convergence to suboptimal policies and stable reduction of policy entropy enables improved trade-off between exploration and exploitation with higher sample efficiency. To address this limitation, we derive influence functions that estimate effect of each sample on policy entropy using the covariance between action probabilities and soft advantages of policies. Building on this, **E2HiL** identifies uninformative samples with extreme values of influence functions, including shortcut samples that induce sharp entropy drops and noisy samples with negligible influence. Rather than treating all samples equally, **E2HiL** further proposes an entropy-bounded sample selection mechanism to prune uninformative samples, which stabilizes policy entropy dynamics, prevents premature collapse. We validate **E2HiL**

¹Nanyang Technological University, Singapore

²Beijing University of Posts and Telecommunications, Beijing, China
† Corresponding author: ziwei.wang@ntu.edu.sg

on four real-world manipulation tasks, where it achieves a 42.1% higher success rate and 10.1% fewer human interventions compared to state-of-the-art HiL-SERL. Extensive experiments results highlight fine-grained entropy regularization as a promising direction for efficient human-in-the-loop real-world RL, enabling policies to reliably acquire robust manipulation skills with significantly fewer human intervention costs.

Our contributions can be summarized as follows:

- 1) We propose **E2HiL**, an efficient real-world human-in-the-loop RL framework that improves sample efficiency by actively selecting informative samples, thereby reducing human intervention costs.
- 2) We characterize sample-induced entropy dynamics through influence functions and apply an entropy-bounded selection rule to remove shortcut and noisy samples, thereby maintaining stable entropy reduction for efficient learning.
- 3) We evaluate **E2HiL** across four real-world tasks and show that its higher sampling efficiency enables faster convergence under reduced human supervision while achieving an effective trade-off between exploration and performance gains.

II. RELATED WORK

A. Real-world RL for Robotic Manipulation

Real-world reinforcement learning (RL) aims to train manipulation policies directly on physical robots, enabling them to acquire skills that operate reliably under real sensor feedback and physical dynamics. However, it remains highly challenging due to issues of sample efficiency [14], [15], [19], sparse rewards [19], [20], and the high cost of human interventions [3], [21]. To address sample inefficiency, prior works have explored off-policy and model-based RL [22], [23], hybrid methods [14], [24], [25], and offline pretraining with foundation-model priors [26]–[28]. Approaches such as reward shaping, inferring rewards from demonstrations or success classifiers [29], [30], and leveraging video-based signals [31] have been proposed to solve the challenge of sparse rewards. To reduce human intervention costs, reset-free learning [32], [33] and autonomous exploration strategies [34] have been introduced. However, these approaches often significantly increase training time and therefore have not achieved widespread adoption in real-world robotic learning. Despite these advances, state-of-the-art methods increasingly adopt HiL-RL, where systems such as HiL-SERL [3] leverage human corrective samples to rapidly acquire precise and dexterous manipulation skills. However, conventional HiL-RL methods treat all intervention samples uniformly, making them unable to distinguish informative guidance from noisy or unhelpful corrections. This leads to inefficient use of human effort and slow policy improvement. In contrast, **E2HiL** addresses this issue by actively selecting the informative samples to guide learning more effectively.

B. Entropy-Regularized Reinforcement Learning

Recent robotic reinforcement learning widely adopts entropy-regularized objectives, most notably through SAC [35], MPO [36] and RLPD [37]. These methods show that entropy bonuses improve exploration and stabilize policy learning in manipulation tasks, but they rely on implicit temperature tuning and do not model entropy at the sample level. Token-level entropy regularization has recently been widely adopted in the training of large language models (LLM) with RL, where regulating entropy dynamics is crucial for balancing exploration and exploitation [38], [39]. Recent studies have proposed methods such as Clip-Higher [18] and staged temperature scheduling [40] to encourage exploration, as well as covariance-based regularizers like Clip-Cov and KL-Cov [17] to mitigate entropy collapse and stabilize learning. In contrast, fine-grained entropy regularization remains largely unexplored in robotic RL, and the fundamental role of entropy in policy learning is still unclear [37]. By analyzing action-level entropy dynamics, we observe patterns similar to those reported in LLM-RL, but with domain-specific differences [41]. To our knowledge, **E2HiL** is the first to introduce sample-level entropy regularization into real-world robotic RL, enabling more sample-efficient learning with faster convergence and reduced human intervention.

III. METHODOLOGY

A. Preliminaries and Problem Statement

We formulate real-world robotic manipulation RL as a Markov Decision Process (MDP) $\mathcal{M} = \{\mathcal{S}, \mathcal{A}, \rho, \mathcal{P}, r, \gamma\}$, where \mathcal{S} denotes the state space (e.g., visual and proprioceptive observations), \mathcal{A} is the action space (e.g., end-effector motions), and $\rho(s_0)$ is the initial state distribution. The transition function $\mathcal{P} : \mathcal{S} \times \mathcal{A} \rightarrow \Delta(\mathcal{S})$ captures the stochastic dynamics of the system, while the reward function $r : \mathcal{S} \times \mathcal{A} \rightarrow \mathbb{R}$ specifies task objectives. The discount factor $\gamma \in [0, 1)$ balances immediate and long-term return. We denote by $s_t \in \mathcal{S}$ and $a_t \in \mathcal{A}$ the state and action at time t .

To enhance real-world training efficiency, we employ human-in-the-loop to improve sample efficiency and utilize RLPD [37] to fully leverage human intervention and exploration samples:

$$\mathcal{L}_Q(\phi) = \mathbb{E}_{(s_t, a_t, r_t, s_{t+1}) \sim \mathcal{D}} \left[(Q_\phi(s_t, a_t) - \hat{y}_t)^2 \right] \quad (1)$$

where the regression target \hat{y}_t is the bootstrapped Bellman target estimating the expected return under the current policy. A slowly updated target network is used to compute \hat{y}_t to stabilize training. In practice, policy is parameterized by neural networks $\pi_\theta(a_t | s_t)$ and the actor parameters θ are updated to maximize the entropy-regularized objective:

$$\mathcal{L}_\pi(\theta) = -\mathbb{E}_{(s_t, a_t) \sim \mathcal{D}} \left[Q_\phi(s_t, a_t) - \alpha \log \pi_\theta(a_t | s_t) \right] \quad (2)$$

where α is an adaptive temperature coefficient controlling the balance between exploitation and exploration.

However, conventional HiL-RL methods [3] uniformly sample from replay buffers with high human intervention

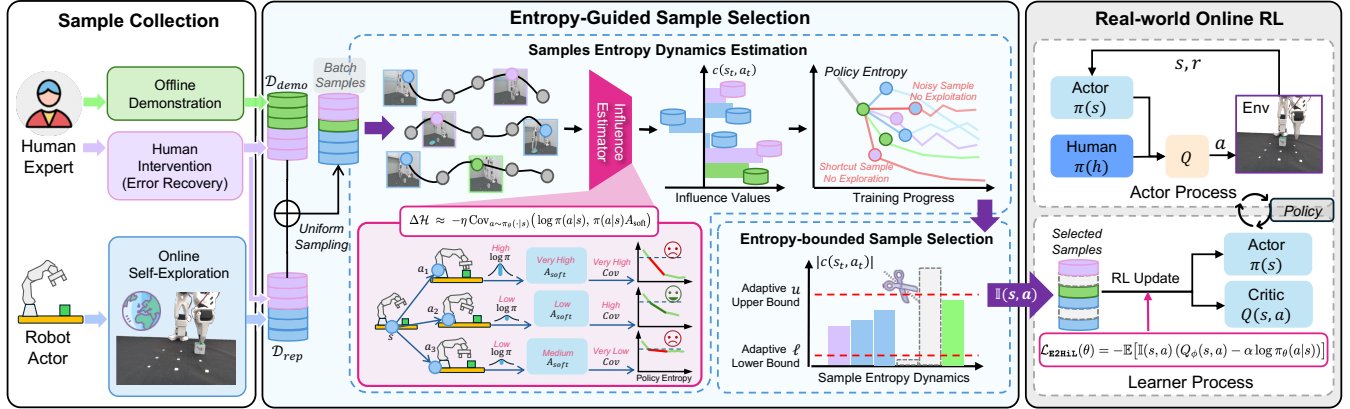


Fig. 2: **Entropy-Guided Sample Selection Framework.** Our framework consists of two key components: Sample Entropy Dynamics Estimation, where we characterize the entropy dynamics induced by each sample, and Entropy-Bounded Sample Selection, where we prune shortcut and noisy samples by constraining their influence value within dynamic bounds.

cost. According to empirical results in [17], stable reduction entropy can improve the exploration and exploitation trade-off with higher sample efficiency, which can reduces the human intervention cost significantly. Therefore, we explicitly formulate our learning objective to incorporate *entropy-guided active sample selection*, wherein training samples contributing to moderate entropy reduction are selected. The objective for HiL-RL is written as follows:

$$\mathcal{L}_{\text{E2HIL}}(\theta) = -\mathbb{E}[\mathbb{I}(s_t, a_t) (Q_\phi(s_t, a_t) - \alpha \log \pi_\theta(a_t | s_t))], \quad (3)$$

where $\mathbb{I}(s_t, a_t) \in \{0, 1\}$ is an indicator function determined by the entropy-bounded selection criterion. Samples with excessive or negligible entropy contribution are masked out ($\mathbb{I} = 0$), removing their gradients from the update. This selective objective preserves only entropy-consistent samples, thereby reducing variance and improving sample efficiency in human-in-the-loop training.

B. Overall Pipeline

Our proposed framework aims to stabilize policy entropy dynamics in human-in-loop RLPD learning by explicitly regulating the selection and use of replay samples during training. As illustrated in Fig. 2, the entire pipeline follows an iterative loop of sample collection, entropy-guided active sample selection, and online RL policy update. For sample collection, **E2HIL** uses three sources: offline demonstrations before training, robot self-exploration samples during online interaction, and human intervention samples which are corrective takeover for error recovery. All collected transitions (s_t, a_t, r_t, s_{t+1}) are stored in the replay buffer \mathcal{D}_{rep} and demonstration buffer $\mathcal{D}_{\text{demo}}$. Before updating the policy, we estimate influence functions of different samples on the policy entropy, which is formulated by influence value $c(s_t, a_t)$: the covariance of action probabilities and soft advantages of policy. Then, we propose entropy-bounded sample selection mechanism that assigns a binary indicator $\mathbb{I}(s_t, a_t)$ to retain samples with moderate influence. Samples with moderate influence on entropy are retained for policy updates, while those causing sharp drops or negligible changes are excluded.

This entropy-guided selection stabilizes entropy dynamics and helps maintain a proper balance between exploration and exploitation. By integrating entropy estimation with selective sampling in a closed training loop, the framework improves sample efficiency and enhances convergence stability in real-world human-in-the-loop RL.

C. Sample Entropy Dynamics Estimation

The key challenge addressed in human-in-the-loop RL is to improve sample efficiency for reducing human intervention cost. Conventional methods treat all samples equally, often causing abrupt entropy reduction and unstable learning. This motivates us to identify informative intervention samples that meaningfully affect policy entropy, which is essential for improving sample efficiency. To address this, we derive batch-wise influence functions that explicitly quantify each sample's effect on entropy dynamics of policy π_θ , which can be approximated by [17]:

$$\Delta\mathcal{H} \approx \mathbb{E}_{s_t \sim d_{\pi_\theta}} \left[-\text{Cov}_{a_t \sim \pi_\theta} (\log \pi_\theta(a_t | s_t), \Delta z_t) \right], \quad (4)$$

where Δz_t denotes the logit change for action a_t at state s_t , d_{π_θ} is the state visitation distribution induced by π_θ , and $\text{Cov}(\cdot, \cdot)$ represents covariance under the action distribution $\pi_\theta(\cdot | s_t)$. Intuitively, by relating policy updates to changes in entropy, Eq. (4) provides a measurable way to assess each sample's influence on policy entropy.

Logit Update under RLPD: To make Eq. (4) applicable in practice, a straightforward approach is to express Δz_t using the actor gradient in RLPD, where policy logits are updated through the standard policy gradient [42]:

$$\Delta z_t := z_t^{t+1} - z_t^t = -\eta \nabla_\theta \mathcal{L}_\pi(\theta) \quad (5)$$

where the negative sign arises from minimizing the RLPD actor objective function \mathcal{L}_π via gradient descent, and η denotes the learning rate. Let $g(s_t, a'_t) \triangleq Q_\phi(s_t, a'_t) - \alpha \log \pi_\theta(a'_t | s_t)$. Here a_t denotes the specific action index associated with the logit parameter θ_{s_t, a_t} , while a'_t denotes actions sampled from the policy $\pi_\theta(\cdot | s_t)$ inside the expectation. Using the

score-function identity, the gradient of the actor objective can be written as:

$$\nabla_{\theta} \mathcal{L}_{\pi}(\theta) = -\pi_{\theta}(a_t | s_t) \left(\underbrace{g(s_t, a_t) - V_{\pi}(s_t)}_{A_{\text{soft}}(s_t, a_t)} \right) \quad (6)$$

See Appendix in project page for full derivation. Here $A_{\text{soft}}(s_t, a_t)$ provides an approximation of the off-policy soft advantage, and $V_{\pi}(s_t)$ is defined as the entropy-regularized state value:

$$V_{\pi}(s_t) := \mathbb{E}_{a'_t \sim \pi_{\theta}} [Q_{\phi}(s_t, a'_t) - \alpha \log \pi_{\theta}(a'_t | s_t)] \quad (7)$$

Eq. (6) naturally appears in RLPD when expressing the policy gradient in terms of the soft advantage, making the actor update depend on the action’s value relative to the entropy-regularized state value. Then we obtain the policy logit change for action a_t at state s_t :

$$\Delta z_t = -\eta \nabla_{\theta} \mathcal{L}_{\pi}(\theta) = \eta \pi_{\theta}(a_t | s_t) A_{\text{soft}}(s_t, a_t) \quad (8)$$

This decomposition expresses logit updates in terms of policy probabilities and soft advantages, enabling a sample-wise characterization of their influence on entropy.

Policy Entropy Change Estimation: Substituting Eq. (8) into Eq. (4), the influence function approximation yields:

$$\Delta \mathcal{H} \approx -\eta \text{Cov}(\log \pi_{\theta}(a_t | s_t), \pi_{\theta}(a_t | s_t) A_{\text{soft}}(s_t, a_t)). \quad (9)$$

which indicates that entropy dynamics are determined by the covariance between action log-probabilities and the soft advantage of policies. This reflects how different samples influence policy entropy: actions with high probability and large soft advantage tend to reduce entropy, while actions with low probability and large soft advantage tend to increase it.

D. Entropy-guided Sample Selection

To stabilize policy entropy and enable more effective utilization of costly human interventions, we propose an *entropy-guided sample selection* framework, consisting of two key components: *sample entropy dynamics estimation* and *entropy-bounded sample selection*.

Sample Entropy Dynamics Estimation: Given a state-action pair (s_t, a_t) , we estimate the covariance term in Eq. (9) via Monte Carlo sampling over the action distribution $\pi_{\theta}(\cdot | s_t)$. Specifically, for each state s_t , we draw K actions $\{a_{t,k}\}_{k=1}^K \sim \pi_{\theta}(\cdot | s_t)$ and compute the empirical covariance between $\log \pi_{\theta}(a_{t,k} | s_t)$ and $\pi_{\theta}(a_{t,k} | s_t) A_{\text{soft}}(s_t, a_{t,k})$. We then define the influence value of sample (s_t, a_t) on entropy dynamics as

$$c(s_t, a_t) \triangleq -\eta \widehat{\text{Cov}}(s_t, a_t). \quad (10)$$

The quantity $c(s_t, a_t)$ is treated as a stop-gradient signal that reflects how this sample contributes to the policy entropy changes.

Entropy-bounded Sample Selection: In practice, we observe that a small portion of samples exhibit extremely large or small covariance magnitudes, far beyond the range of the majority within the same batch. These outlier samples

Algorithm 1 RL with Entropy-guided Sample Selection

```

Temperature  $\alpha$ , gradient steps  $G$ , batch size  $N$ 
Initialize critics  $\phi_i$  (targets  $\phi'_i \leftarrow \phi_i$ ); initialize actor  $\theta$ 
Initialize replay buffer  $\mathcal{D}_{\text{rep}}$  and demo buffer  $\mathcal{D}_{\text{demo}}$ 
Receive initial state  $s_0$ 
for  $t = 0$  to  $T$  do
  if human intervention then
    Take action  $a_t$  from human operator
    Store  $(s_t, a_t, r_t, s_{t+1})$  in  $\mathcal{D}_{\text{rep}}$  and  $\mathcal{D}_{\text{demo}}$ 
  else
    Sample  $a_t \sim \pi_{\theta}(\cdot | s_t)$ 
    Store  $(s_t, a_t, r_t, s_{t+1})$  in  $\mathcal{D}_{\text{rep}}$ 
  for  $g = 1$  to  $G$  do
    Sample minibatch  $b_R$  of  $N/2$  from  $\mathcal{D}_{\text{rep}}$ 
    Sample minibatch  $b_D$  of  $N/2$  from  $\mathcal{D}_{\text{demo}}$ 
    Set  $b \leftarrow b_R \cup b_D$ 
    Update  $\phi$  minimizing loss from Eq. (1):
    Update target networks  $\phi'_i \leftarrow \rho \phi'_i + (1 - \rho) \phi_i$ 
  Estimate influence value  $c_i$  on  $b$  from Eq. (10)
  Get indicator function  $\mathbb{I}(s_t, a_t)$  from Eq. (11)
  Update actor by maximizing objective Eq. (12)

```

play a dominant role in triggering abnormal entropy fluctuations, which can either drive the policy into premature collapse or stall its progress. Concretely, we categorize some problematic samples: (1) shortcut samples that induce abrupt entropy drops and cause premature policy collapse, and (2) noisy samples that contribute negligibly to entropy change and slow down learning progress (see Sec. IV-C for empirical verification). To mitigate the impact of samples that cause abrupt entropy changes or contribute negligibly to exploration, we clip the estimated absolute influence value $\{|c(s_t, a_t)|\}$ within a dynamically adjusted interval $[\ell, u]$, where the bounds are computed adaptively from the batch-wise percentile range of influence magnitudes. Formally, we define an indicator function that determines whether a sample participates in the policy update:

$$\mathbb{I}(s_t, a_t) = \mathbf{1} [|c(s_t, a_t)| \in [\ell, u]]. \quad (11)$$

Samples outside this range are masked out ($\mathbb{I} = 0$), effectively canceling their gradient contributions. Given the per-sample actor loss $l_t := Q_{\phi}(s_t, a_t) - \alpha \log \pi_{\theta}(a_t | s_t)$, our entropy-aware actor objective is defined as:

$$\mathcal{L}_{\text{E2HiL}}(\theta) = -\frac{\sum_{(s_t, a_t) \in \mathcal{B}} \mathbb{I}(s_t, a_t) l_t}{\sum_{(s_t, a_t) \in \mathcal{B}} \mathbb{I}(s_t, a_t) + \varepsilon} \quad (12)$$

where \mathcal{B} denotes a minibatch of size B , and ε is a small constant for numerical stability. This formulation ensures that only entropy-consistent samples contribute to the gradient, leading to smoother entropy evolution and more stable convergence in human-in-the-loop training.

IV. EXPERIMENTS

In this section, we first present the real-world experimental setups. We then report the performance of **E2HiL** in compar-

TABLE I: **Real-world Results.** Comparison of success rate and intervention rate between **E2HiL** and HIL-SERL [3] across four tasks.

	Method	Touch Cube	Pick Cube	Pick & Place Cube	Stack Blocks	Average
Success Rate (%) \uparrow	HIL-SERL	55.4	40.0	36.1	35.7	41.8
	E2HiL	92.5	93.2	71.3	78.7	83.9
Intervention Rate (%) \downarrow	HIL-SERL	42.6	39.9	41.4	52.1	44.0
	E2HiL	23.3	31.4	37.1	43.6	33.9

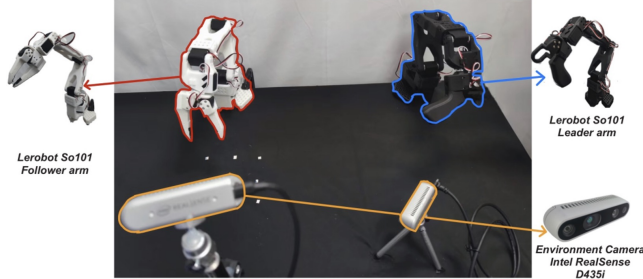


Fig. 3: **Real-world robot setup.** We employ the Lerobot SO-101 as our real-world reinforcement learning platform.

ison with state-of-the-art HiL-RL method. Next, we evaluate the accuracy of our estimation of sample-induced entropy dynamics and verify the reliability of the proposed entropy-guided sample selection mechanism. We then analyze the distribution and characteristics of the pruned shortcut and noisy samples, and further examine how different types of human interventions influence policy learning in real-world robotic manipulation.

A. Experimental Setup

Real Robot. As illustrated in Fig. 3, we employ the *lerobot SO101 leader-follower* robotic system as our real-world reinforcement learning platform [43]. In this setup, the *SO101 follower* serves as the RL actor agent that interacts with the environment, while the *SO101 leader* provides a homomorphic mapping interface for human interventions. This design allows human operators to directly influence the policy execution through the leader robot, enabling efficient corrective feedback during training. For robot observations, we employ RGB images from two cameras with a resolution of 128×128 at 30 Hz. Additionally, 10 real-world human demonstrations are collected via leader-robot teleoperation to initialize the demonstration buffer $\mathcal{D}_{\text{demo}}$, which provides informative priors that help stabilize early training and accelerate policy convergence [37].

Baseline. We adopt HIL-SERL [3] as our baseline, the state-of-the-art human-in-the-loop RL method for real-world manipulation. HIL-SERL trains the manipulation policy from scratch and integrates corrective human interventions into the learning process, while additionally incorporating the entropy regularization from RLPD to stabilize policy updates. Our implementation is built on top of the lerobot framework [43].

Evaluation Metrics. We report three main metrics: the final **success rate** and the average **human intervention**

rate. The human intervention rate is defined as the ratio between the number of intervention steps and the total robot interaction steps. We also monitor the evolution of the **policy entropy curve** to evaluate the stability of learning and the quality of exploration.

B. Comparisons with the State-of-the-Art

General Comparison. We compare **E2HiL** with the state-of-the-art human-in-the-loop RL method HIL-SERL and report the performances across four position-generalization tasks of increasing difficulty. As shown in Fig. 4, **E2HiL** achieves the best performance in terms of convergence success rate, average human intervention rate, and the stability of the entropy curve. These results demonstrate that entropy-guided sample selection mechanism not only improves task performance and reduces human effort, but also stabilizes the entropy dynamics during training. From Table I, we observe that **E2HiL** achieves a sizable relative improvement of **42.1%** in success rate across four tasks, while reducing the average human intervention rate by **10.1%**. Moreover, **E2HiL** requires only 68.7k steps on average to reach a 70% success rate across four tasks, whereas HIL-SERL prematurely converges to suboptimal performance due to aggressive entropy collapse. These consistent gains demonstrate the effectiveness of entropy-guided sample selection mechanism in improving task performance, reducing human effort, and stabilizing real-world RL training.

Case Study Analysis. Fig. 4 shows a case study focusing on the *Touch-Cube* task. For stable learning and fair comparison, the cube is randomly placed at either position 1 or position 2 during training to prevent the policy from overfitting to a single location. This setup ensures that the agent must discover both skills (touching at position 1 and position 2) through interaction, allowing us to evaluate both learning efficiency and generalization capability. Both **E2HiL** and the HIL-SERL baseline exhibit an initial entropy reduction as the policy learns the first position. However, **E2HiL** clips out shortcut samples that cause abrupt entropy drops, resulting in a more moderate entropy decrease. By leveraging human intervention samples more effectively, **E2HiL** successfully acquires the first skill at around 10k steps. Crucially, **E2HiL** maintains exploration capacity because entropy does not collapse prematurely and learns to locate the second cube position at approximately 20k steps. With continued human corrections, it eventually acquires the second position at about 33k steps, converging more slowly and with higher human cost than **E2HiL**.

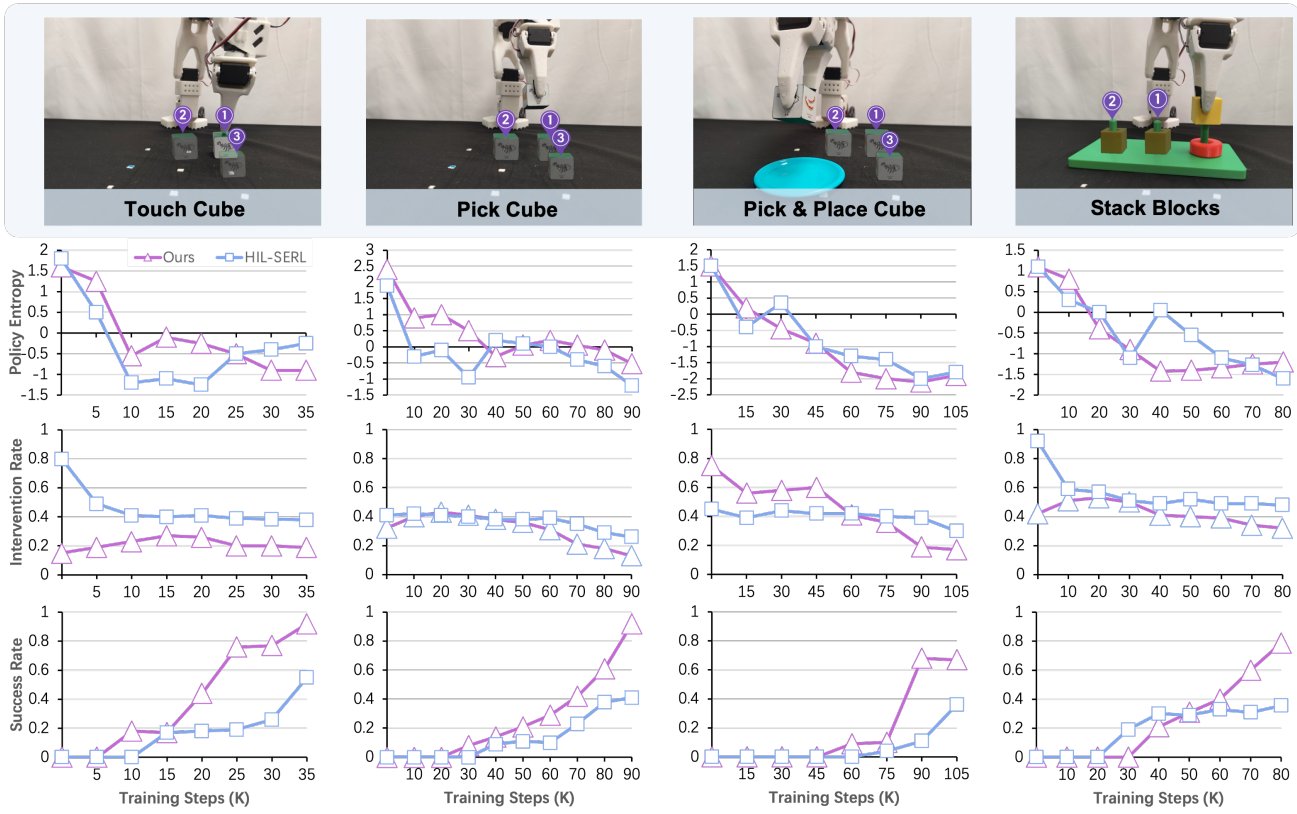


Fig. 4: **Comparison with Baseline.** **E2Hil** significantly outperforms state-of-the-art human-in-the-loop RL approaches by achieving higher success rates and requiring fewer human interventions across four tasks. With entropy-guided sample selection, **E2Hil** further exhibits more stable entropy dynamics, avoiding premature entropy collapse and ineffective updates.

C. Analysis of Samples Entropy Dynamics

Empirical Verification. A natural question arises from the previous results: *how effective is our estimation of the contribution of samples to policy entropy change?* To answer this, we empirically validate our core result that sample-induced entropy dynamics can be accurately characterized through the covariance between action log-probabilities and soft advantages of policy, as formulated in Eq. (9). Concretely, during the training process of HIL-SERL for the *Touch-Cube* task, we compute the batch-wise average covariance $\text{Cov}(\cdot)$ of samples at every policy update and compare it with the ground-truth entropy derivative $-\Delta H$. As shown in Fig. 5 Left, the two curves exhibit a strong proportional relationship, consistent with our theoretical formulation. This alignment is especially pronounced during the initial entropy reduction phase (0–10k steps) and the subsequent entropy increase (10k–20k steps). As training progresses beyond 20k steps, where policy entropy stabilizes, the covariance values fluctuate closely around zero, further supporting the validity of our estimation. However, we also observe deviations in the first 5k steps, likely due to inaccurate Q-value estimates from the critic, leading to biased A_{soft} computation in Eq. 9. Future work may incorporate calibration techniques such as Cal-QL [44] to improve Q-value reliability before online training.

Human Intervention Sample Analysis. Having verified the accuracy of our characterization of sample-induced en-

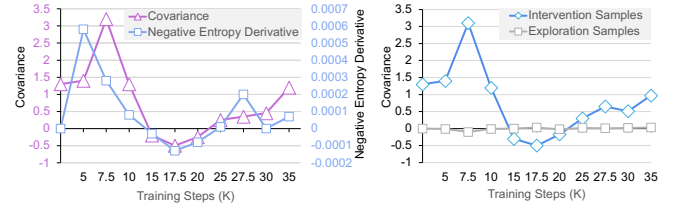


Fig. 5: *Left:* The policy entropy derivative and covariance during human-in-the-loop RL training in the *Touch-Cube* task. *Right:* Covariance of human intervention samples and policy self-exploration samples.

tropy dynamics, we next analyze how human intervention samples and self-exploration samples differ in their influence on policy learning under real-world HiL-RL. During the HIL-SERL training process for the *Touch-Cube* task, we compute the per-sample covariance c_i and attach tracking tags to samples originating from human interventions. As illustrated in Fig. 5 Right, human intervention samples exhibit significantly higher amplitudes and larger mean covariance values compared to self-exploration samples, indicating that they contribute more strongly to policy entropy change. This observation is further corroborated in Table II, which reports the distribution of covariance magnitudes across all samples, as well as within the human intervention and self-exploration subsets. The results show that human intervention samples overwhelmingly populate the upper tail of the covariance distribution, playing a decisive role in driving

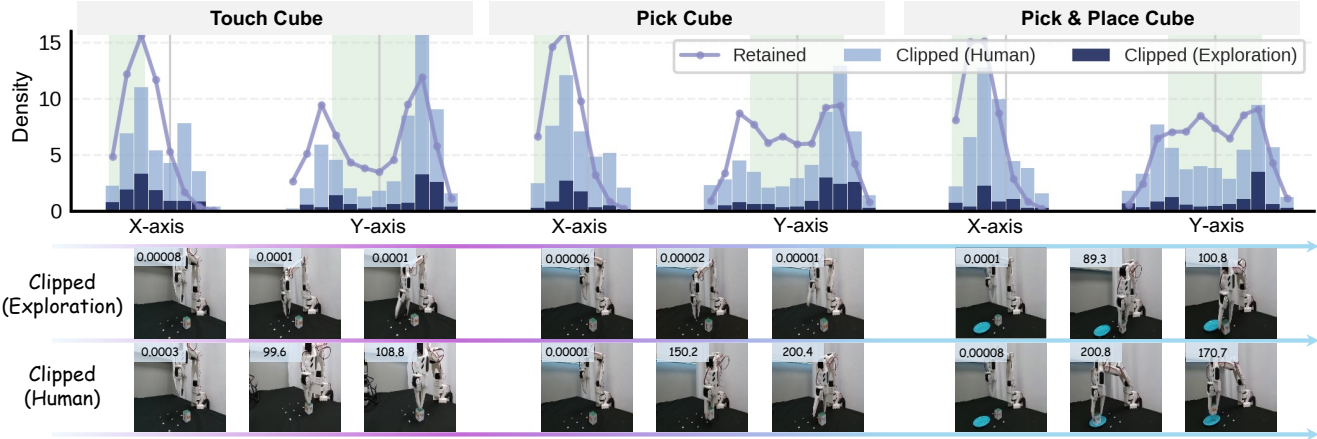


Fig. 6: **Retained vs. Clipped Sample Distribution in Three Tasks.** Line density of retained samples and histogram of clipped samples shown in task space (gripper position). Most clipped samples come from human interventions, and their covariance visualization highlights out-of-workspace or redundant states.

TABLE II: **Samples Covariance Distribution.** Mean absolute covariance across different sample types.

Subset	All Samples	Intervention Samples	Exploration Samples
Top 2%	269.9	368.1	5.56
Top 5%	127.0	180.2	2.7
Top 10%	67.3	98.6	1.5
Top 20%	34.2	51.1	0.8
Top 50%	13.8	20.6	0.3
Low 20%	0.001	0.002	0.0007
Low 10%	0.0005	0.0007	0.0003
Low 5%	0.0002	0.0003	0.0001
Low 2%	0.00008	0.0001	0.00006
All	6.9	10.3	0.2

policy entropy dynamics, which accelerate the early stages of policy improvement. However, both types of samples also exhibit distinct forms of instability. In particular, we observe that the extreme values in the covariance distribution come from two problematic sample types: (i) *shortcut samples* that induce sharp entropy drops and risk premature policy collapse, and (ii) *noisy samples* with near-zero covariance that contribute negligibly to entropy change and impede learning progress. These observations motivate our dynamically adjusted clipping interval $[\ell, u]$, where the bounds are determined adaptively for each batch as the 5th and 90th percentiles of $\{|c(s_t, a_t)|\}$.

D. Analysis of Clipped Samples

Finally, we analyze the distribution and characteristics of the clipped samples, and provide insights into the potential mechanisms by which human intervention influences real-world RL training. Fig. 6 visualizes the sampling selection results. During **E2HIL** training, we retained an equal number of clipped and retained samples at each training step, accumulated them over time, and scaled their counts proportionally to the intensity shown in the figure. Specifically, the retained samples are shown as a line plot, while the clipped samples are illustrated using histograms. Interestingly, we find that the majority of clipped samples originate from human intervention samples. To better interpret their spatial distribution, we overlay the task-aware workspace of the manipulator. The visualization shows that most samples lying

outside the designated workspace, namely states beyond the robot’s effective manipulation region, are removed. This indicates that the entropy-bounded sample selection mechanism filters out transitions that contribute little meaningful gradient information for task learning. Moreover, even within the workspace, a subset of samples is pruned. Further inspection of the clipped samples reveals that many correspond to redundant or repeated states, which offer minimal contribution to entropy dynamics and may slow down policy improvement. This observation suggests that entropy-bounded sample clipping not only prevents shortcut samples from collapsing exploration but also reduces the impact of noisy, low-diversity corrections, thereby facilitating more stable policy learning.

V. CONCLUSION

In this paper, we proposed an efficient real-world human-in-the-loop RL framework named **E2HIL**, featuring an entropy-guided sample selection mechanism. By characterizing sample-induced entropy dynamics through covariance-based influence functions, we identify shortcut and noisy samples that hinder learning. Our entropy-bounded selection mechanism removes these uninformative samples, maintaining stable entropy evolution and enabling more efficient policy updates with minimal human intervention. Real-world experiments across multiple tasks show that our method achieves higher success rates with fewer human interventions than the state-of-the-art baseline while achieving an effective trade-off between exploration and performance gains.

In future work, we plan to extend **E2HIL** to scalable multi-task real-world reinforcement learning for vision-language-action (VLA) models and enhance covariance estimation by adopting more reliable value estimation techniques for improved stability and sample efficiency.

REFERENCES

- [1] J. F. Buhl, R. Grønhøj, J. K. Jørgensen, G. Mateus, D. Pinto, J. K. Sørensen, S. Bøgh, and D. Chrysostomou, “A dual-arm collaborative robot system for the smart factories of the future,” *Procedia manufacturing*, vol. 38, pp. 333–340, 2019.

[2] T. Zhang, D. Li, Y. Li, Z. Zeng, L. Zhao, L. Sun, Y. Chen, X. Wei, Y. Zhan, L. Li, *et al.*, “Empowering embodied manipulation: A bimanual-mobile robot manipulation dataset for household tasks,” *arXiv preprint arXiv:2405.18860*, pp. 1–24, 2024.

[3] J. Luo, C. Xu, J. Wu, and S. Levine, “Precise and dexterous robotic manipulation via human-in-the-loop reinforcement learning,” *Science Robotics*, pp. 1–54, 2025.

[4] T. Z. Zhao, J. Tompson, D. Driess, P. Florence, K. Ghasemipour, C. Finn, and A. Wahid, “Aloha unleashed: A simple recipe for robot dexterity,” 2024, pp. 1–17.

[5] O. Kroemer, S. Niekum, and G. Konidaris, “A review of robot learning for manipulation: Challenges, representations, and algorithms,” *Journal of machine learning research*, vol. 22, no. 30, pp. 1–82, 2021.

[6] V. Saxena, M. Bronars, N. R. Arachchige, K. Wang, W. C. Shin, S. Nasiriany, A. Mandlekar, and D. Xu, “What matters in learning from large-scale datasets for robot manipulation,” in *The Thirteenth International Conference on Learning Representations (ICLR)*, 2025.

[7] H. Deng, Z. Wu, H. Liu, W. Guo, Y. Xue, Z. Shan, C. Zhang, B. Jia, Y. Ling, G. Lu, *et al.*, “A survey on reinforcement learning of vision-language-action models for robotic manipulation,” *Authorea Preprints*, 2025.

[8] G. Lu, W. Guo, C. Zhang, Y. Zhou, H. Jiang, Z. Gao, Y. Tang, and Z. Wang, “Vla-rl: Towards masterful and general robotic manipulation with scalable reinforcement learning,” *arXiv preprint arXiv:2505.18719*, 2025.

[9] C.-Y. Hung, N. Majumder, H. Deng, L. Renhang, Y. Ang, A. Zadeh, C. Li, D. Herremans, Z. Wang, and S. Poria, “Nora-1.5: A vision-language-action model trained using world model-and action-based preference rewards,” *arXiv preprint arXiv:2511.14659*, 2025.

[10] W. Guo, G. Lu, H. Deng, Z. Wu, Y. Tang, and Z. Wang, “Vla-reasoner: Empowering vision-language-action models with reasoning via online monte carlo tree search,” *arXiv preprint arXiv:2509.22643*, 2025.

[11] E. Salvato, G. Fenu, E. Medvet, and F. A. Pellegrino, “Crossing the reality gap: A survey on sim-to-real transferability of robot controllers in reinforcement learning,” *IEEE Access*, vol. 9, pp. 153 171–153 187, 2021.

[12] M. Yang, Y. Lin, A. Church, J. Lloyd, D. Zhang, D. A. Barton, and N. F. Lepora, “Sim-to-real model-based and model-free deep reinforcement learning for tactile pushing,” *IEEE Robotics and Automation Letters*, vol. 8, no. 9, pp. 5480–5487, 2023.

[13] L. Chen, Y. Lei, S. Jin, Y. Zhang, and L. Zhang, “Rlingua: Improving reinforcement learning sample efficiency in robotic manipulations with large language models,” *IEEE Robotics and Automation Letters*, vol. 9, no. 7, pp. 6075–6082, 2024.

[14] T. Zhang and H. Mo, “Reinforcement learning for robot research: A comprehensive review and open issues,” *International Journal of Advanced Robotic Systems*, 2021.

[15] M. Torne, A. Simeonov, Z. Li, A. Chan, T. Chen, A. Gupta, and P. Agrawal, “Reconciling reality through simulation: A real-to-sim-to-real approach for robust manipulation,” *arXiv preprint arXiv:2403.03949*, pp. 1–23, 2024.

[16] A. Muraleedharan *et al.*, “Selective progress-aware querying for human-in-the-loop reinforcement learning,” *arXiv preprint arXiv:2509.20541*, 2025.

[17] G. Cui, Y. Zhang, J. Chen, L. Yuan, Z. Wang, Y. Zuo, H. Li, Y. Fan, H. Chen, W. Chen, *et al.*, “The entropy mechanism of reinforcement learning for reasoning language models,” *arXiv preprint arXiv:2505.22617*, 2025.

[18] H. Li, Y. Zuo, J. Yu, Y. Zhang, Z. Yang, K. Zhang, X. Zhu, Y. Zhang, T. Chen, G. Cui, *et al.*, “Simplevla-rl: Scaling vla training via reinforcement learning,” *arXiv preprint arXiv:2509.09674*, 2025.

[19] H. Ju, R. Juan, R. Gomez, K. Nakamura, and G. Li, “Transferring policy of deep reinforcement learning from simulation to reality for robotics,” *Nature Machine Intelligence*, vol. 4, pp. 1077–1087, 2022.

[20] C. Tang, B. Abbatematteo, J. Hu, R. Chandra, R. Martín-Martín, and P. Stone, “Deep reinforcement learning for robotics: A survey of real-world successes,” in *Proceedings of the AAAI Conference on Artificial Intelligence (AAAI)*, vol. 39, no. 27, 2025, pp. 28 694–28 698.

[21] J. Spencer, S. Choudhury, M. Barnes, M. Schmittie, M. Chiang, P. Ramadge, and S. Srinivasa, “Expert intervention learning: An online framework for robot learning from explicit and implicit human feedback,” *Autonomous Robots*, vol. 46, no. 1, pp. 99–113, 2022.

[22] I. Clavera, J. Röthfuss, J. Schulman, Y. Fujita, T. Asfour, and P. Abbeel, “Model-based reinforcement learning via meta-policy optimization,” in *Conference on Robot Learning (CoRL)*, 2018, pp. 617–629.

[23] M. A. Lee, C. Florensa, J. Tremblay, N. Ratliff, A. Garg, F. Ramos, and D. Fox, “Guided uncertainty-aware policy optimization: Combining learning and model-based strategies for sample-efficient policy learning,” in *2020 IEEE international conference on robotics and automation (ICRA)*, 2020, pp. 7505–7512.

[24] A. Pinosky, I. Abraham, A. Broad, B. Argall, and T. D. Murphey, “Hybrid control for combining model-based and model-free reinforcement learning,” *International Journal of Robotics Research (IJRR)*, vol. 42, no. 6, pp. 337–355, 2023.

[25] K. Lei, H. Li, D. Yu, Z. Wei, L. Guo, Z. Jiang, Z. Wang, S. Liang, and H. Xu, “Rl-100: Performant robotic manipulation with real-world reinforcement learning,” *arXiv preprint arXiv:2510.14830*, 2025.

[26] F. Zhong, K. Wu, H. Ci, C. Wang, and H. Chen, “Empowering embodied visual tracking with visual foundation models and offline rl,” in *European Conference on Computer Vision (ECCV)*. Springer, 2024, pp. 139–155.

[27] M. Kelly, C. Sidrane, K. Driggs-Campbell, and M. J. Kochenderfer, “Hg-dagger: Interactive imitation learning with human experts,” in *2019 International Conference on Robotics and Automation (ICRA)*. IEEE, 2019, pp. 8077–8083.

[28] K. Kawaharazuka, T. Matsushima, A. Gambardella, J. Guo, C. Paxton, and A. Zeng, “Real-world robot applications of foundation models: A review,” *Advanced Robotics*, vol. 38, no. 18, pp. 1232–1254, 2024.

[29] R. Devidze, P. Kamalaruban, and A. Singla, “Exploration-guided reward shaping for reinforcement learning under sparse rewards,” *Advances in Neural Information Processing Systems (NeurIPS)*, vol. 35, pp. 5829–5842, 2022.

[30] F. Memarian, W. Goo, R. Lioutikov, S. Niekum, and U. Topcu, “Self-supervised online reward shaping in sparse-reward environments,” in *2021 IEEE/RSJ International Conference on Intelligent Robots and Systems (IROS)*. IEEE, 2021, pp. 2369–2375.

[31] Y. Cao, H. Zhao, Y. Cheng, T. Shu, Y. Chen, G. Liu, G. Liang, J. Zhao, J. Yan, and Y. Li, “Survey on large language model-enhanced reinforcement learning: Concept, taxonomy, and methods,” *IEEE Transactions on Neural Networks and Learning Systems*, 2024.

[32] A. Gupta, J. Yu, T. Z. Zhao, V. Kumar, A. Rovinsky, K. Xu, T. Devlin, and S. Levine, “Reset-free reinforcement learning via multi-task learning: Learning dexterous manipulation behaviors without human intervention,” in *2021 IEEE International Conference on Robotics and Automation (ICRA)*. IEEE, 2021, pp. 6664–6671.

[33] Z. Yang, T. M. Moerland, M. Preuss, A. Plaat, and E. S. Hu, “Reset-free reinforcement learning with world models,” *arXiv preprint arXiv:2408.09807*, 2024.

[34] R. Dromnelle, E. Renaudo, M. Chetouani, P. Maragos, R. Chatila, B. Girard, and M. Khamassi, “Reducing computational cost during robot navigation and human–robot interaction with a human-inspired reinforcement learning architecture,” *International Journal of Social Robotics*, vol. 15, no. 8, pp. 1297–1323, 2023.

[35] T. Haarnoja, A. Zhou, P. Abbeel, and S. Levine, “Soft actor-critic: Off-policy maximum entropy deep reinforcement learning with a stochastic actor,” in *Proceedings of Machine Learning Research*, vol. 80. PMLR, 2018, pp. 1861–1870.

[36] A. Abdolmaleki, J. T. Springenberg, Y. Tassa, R. Munos, N. Heess, and M. Riedmiller, “Maximum a posteriori policy optimisation,” *arXiv preprint arXiv:1806.06920*, 2018.

[37] P. J. Ball, L. Smith, I. Kostrikov, and S. Levine, “Efficient online reinforcement learning with offline data,” in *Proceedings of the International Conference on Machine Learning (ICML)*. PMLR, 2023, pp. 1577–1594.

[38] D. Cheng, S. Huang, X. Zhu, B. Dai, W. X. Zhao, Z. Zhang, and F. Wei, “Reasoning with exploration: An entropy perspective,” *arXiv preprint arXiv:2506.14758*, 2025.

[39] D. Tiapkin, D. Belomestny, D. Calandriello, E. Moulines, R. Munos, A. Naumov, P. Perrault, Y. Tang, M. Valko, and P. Menard, “Fast rates for maximum entropy exploration,” in *Proceedings of the International Conference on Machine Learning (ICML)*. PMLR, 2023, pp. 34 161–34 221.

[40] M. Renze, “The effect of sampling temperature on problem solving in large language models,” in *Findings of the association for computational linguistics: EMNLP 2024*, 2024, pp. 7346–7356.

[41] B. Eysenbach and S. Levine, “Maximum entropy rl (provably) solves some robust rl problems,” *arXiv preprint arXiv:2103.06257*, 2021.

- [42] R. J. Williams, “Simple statistical gradient-following algorithms for connectionist reinforcement learning,” *Machine learning*, vol. 8, no. 3, pp. 229–256, 1992.
- [43] R. Cadene, S. Alibert, A. Soare, Q. Gallooudec, A. Zouitine, S. Palma, P. Kooijmans, M. Aractingi, M. Shukor, D. Aubakirova, M. Russi, F. Capuano, C. Pascal, J. Choghari, J. Moss, and T. Wolf, “Lerobot: State-of-the-art machine learning for real-world robotics in pytorch,” <https://github.com/huggingface/lerobot>, 2024.
- [44] M. Nakamoto, S. Zhai, A. Singh, M. Sobol Mark, Y. Ma, C. Finn, A. Kumar, and S. Levine, “Cal-ql: Calibrated offline rl pre-training for efficient online fine-tuning,” *Proceedings of Advances in Neural Information Processing Systems*, vol. 36, pp. 62 244–62 269, 2023.